Appendix S1. Supplemental methods

Functional test for pendrin ion transport. The ion transport function of pendrin was measured via a fluorometric method allowing for evaluation of iodide influx in pendrin-transfected cells (1-11). In detail, cells were initially washed and bathed in 70 μl of a high-chloride solution (in mM: KCl 2, NaCl 135, $CaCl_2$ 1, $MgCl_2$ 1, D-glucose 10, 4-(2-hydroxyethyl)-1-piperazineethane sulfonic acid (HEPES) 20, 308 mOsm/KgH_2O adjusted with mannitol, pH 7.4), and the baseline fluorescence intensity was measured (1 measurement/sec for 3 sec). Subsequently, 140 μl of a high-iodide solution (in mM: KCl 2, NaI 135, $CaCl_2$ 1, $MgCl_2$ 1, D-glucose 10, HEPES 20, 308 mOsm/KgH_2O adjusted with mannitol, pH 7.4) were injected into each well and the fluorescence intensity was followed for 16 sec. Fluorescence intensity was quantified with the VICTOR™ X3 Multilabel Plate Reader (Perkin Elmer, Inc.) equipped with a liquid dispenser and the following filters: excitation: F485 (excitation center wavelength: 485 nm, bandwidth: 14 nm), emission: F535 (emission center wavelength: 535 nm, bandwidth: 25 nm). The background fluorescence was subtracted from all of the other fluorescence measurements of the same 96-well plate. Data are expressed as % fluorescence variations and a negative fluorescence variation indicates a flux of iodide from the extracellular milieu to the intracellular environment. Experiments were performed at room temperature.

Determination of total protein expression levels by quantitative imaging. Quantitative imaging was performed as formerly described (2,9). Specifically, HeLa cells expressing wild-type or mutant SLC26A4-EYFP were fixed with 4% paraformaldehyde for 30 min, counterstained with 0.1 μg/ml 4',6-diamidino-2-phenylindole (DAPI) for 10 min, thoroughly washed and imaged in Hank's balanced salt solution (HBSS; MilliporeSigma). Imaging was performed with a Leica TCS SP5II AOBS confocal microscope (Leica Microsystems GmbH) equipped with an HCX PL APO 63x/1.20 Lambda blue water immersion objective and controlled by the LAS AF SP5 software version 2.7.3.9723 (Leica Microsystems GmbH). EYFP was excited with the 514 nm line of the Argon laser and emission was detected between 525 and 600 nm; DAPI was excited with a diode laser (405 nm) and emission was detected between 430 and 470 nm. Laser power and photomultipliers gain were kept rigorously constant for the acquisition of all images. To normalize pendrin expression levels for the cell density, the EYFP fluorescence intensity of whole imaging fields was expressed as average levels of gray, subtracted for the background fluorescence, and normalized for the background-subtracted fluorescence intensity of DAPI.

Determination of protein expression levels in the plasma membrane region. For the determination of protein expression levels in the plasma membrane region, a formerly optimized protocol was utilized (9). Living HeLa cells expressing wild-type or mutant SLC26A4-EYFP and ECFP were stained with 1.25 μg/ml CellMask™ Deep Red plasma membrane stain (cat. no. C10046; Molecular Probes; Thermo Fisher Scientific, Inc.) in HBSS for 5 min on ice, thoroughly washed, and imaged in HBSS. To normalize protein expression for the transfection efficiency of the single cell, the EYFP fluorescence intensity of three regions of interest (ROIs) of the plasma membrane of a single cell was subtracted for the background fluorescence, averaged, and normalized for the background-subtracted ECFP fluorescence intensity measured in the cytosol of the same cell. The choice of the ROIs was guided by the plasma membrane stain. Imaging was performed by confocal microscopy as aforementioned. EYFP was excited with the 514 nm line of the Argon laser and emission was detected between 525 and 580 nm. ECFP was excited with a diode laser (405 nm) and emission was detected between 450 and 490 nm. CellMask™ Deep Red stain was excited at 633 nm (HeNe laser) and emission was detected in the 643-750 nm range. Laser power and photomultipliers gain were kept rigorously constant for the acquisition of all images.

Western blotting. Proteins (20 μg) were solubilized in a 4X loading dye containing 100 mM dithiothreitol and 8% SDS, separated on a 7.5% polyacrylamide gel containing 0.1% SDS, and electroblotted on a polyvinylidene fluoride (PVDF) membrane (Bio-Rad Laboratories, Inc.) by applying a constant voltage (75 V) for 2 h at 4˚C. Except where otherwise specified, PVDF membranes were blocked for 1 h at room temperature in 5% non-fat dry milk diluted in Tris-buffered saline (137 mM NaCl and 20 mM Tris-HCl) containing 0.1% Tween 20 (TBST) and incubated overnight at 4˚C or for one hour at room temperature with the primary or the secondary antibodies, respectively, all diluted in TBST and 5% non-fat dry milk.

Mass spectrometry. Full-spectrum MS scans of the separated peptides were performed between 300-1,650 m/z at the resolution 60,000 at 200 m/z, and the automatic gain control target for the full scan was set to $3x10^6$. The MS/MS scan was operated in Top 20 mode using the following settings: resolution 15,000 at 200 m/z, automatic gain control target $1x10^5$, maximum injection time 19 ms, normalized collision energy at 28%, isolation window of 1.4 Th, dynamic exclusion 30 sec (Creative Proteomics).

References

1. Matulevicius A, Bernardinelli E, Brownstein Z, Roesch S, Avraham KB and Dossena S: Molecular features of SLC26A4 common variant p.L117F. J Clin Med 11: 5549, 2022.
2. Roesch S, Bernardinelli E, Nofziger C, Tóth M, Patsch W, Rasp G, Paulmichl M and Dossena S: Functional testing of SLC26A4 variants-clinical and molecular analysis of a cohort with enlarged vestibular aqueduct from Austria. Int J Mol Sci 19: 209, 2018.
3. Procino G, Milano S, Tamma G, Dossena S, Barbieri C, Nicoletti MC, Ranieri M, Di Mise A, Nofziger C, Svelto M, *et al*: Co-regulated pendrin and aquaporin 5 expression and trafficking in Type-B intercalated cells under potassium depletion. Cell Physiol Biochem 32: 184-199, 2013.
4. Pera A, Dossena S, Rodighiero S, Gandía M, Bottà G, Meyer G, Moreno F, Nofziger C, Hernández-Chico C and Paulmichl M: Functional assessment of allelic variants in the SLC26A4 gene involved in Pendred syndrome and nonsyndromic EVA. Proc Natl Acad Sci USA 105: 18608-18613, 2008.
5. Fugazzola L, Cirello V, Dossena S, Rodighiero S, Muzza M, Castorina P, Lalatta F, Ambrosetti U, Beck-Peccoz P, Bottà G and Paulmichl M: High phenotypic intrafamilial variability in patients with Pendred syndrome and a novel duplication in the SLC26A4 gene: Clinical characterization and functional studies of the mutated SLC26A4 protein. Eur J Endocrinol 157: 331-338, 2007.

6. Dror AA, Politi Y, Shahin H, Lenz DR, Dossena S, Nofziger C, Fuchs H, Hrabé de Angelis M, Paulmichl M, Weiner S and Avraham KB: Calcium oxalate stone formation in the inner ear as a result of an Slc26a4 mutation. J Biol Chem 285: 21724-21735, 2010.
7. Dossena S, Bizhanova A, Nofziger C, Bernardinelli E, Ramsauer J, Kopp P and Paulmichl M: Identification of allelic variants of pendrin (SLC26A4) with loss and gain of function. Cell Physiol Biochem 28: 467-476, 2011.
8. Dossena S, Nofziger C, Brownstein Z, Kanaan M, Avraham KB and Paulmichl M: Functional characterization of pendrin mutations found in the Israeli and Palestinian populations. Cell Physiol Biochem 28: 477-484, 2011.
9. de Moraes VCS, Bernardinelli E, Zocal N, Fernandez JA, Nofziger C, Castilho AM, Sartorato EL, Paulmichl M and Dossena S: Reduction of cellular expression levels is a common feature of functionally affected pendrin (SLC26A4) protein variants. Mol Med 22: 41-53, 2016.
10. Bernardinelli E, Costa R, Nofziger C, Paulmichl M and Dossena S: Effect of known inhibitors of Ion transport on pendrin (SLC26A4) activity in a human kidney cell line. Cell Physiol Biochem 38: 1984-1998, 2016.
11. Dossena S, Rodighiero S, Vezzoli V, Bazzini C, Sironi C, Meyer G, Fürst J, Ritter M, Garavaglia ML, Fugazzola L, *et al:* Fast fluorometric method for measuring pendrin (SLC26A4) Cl-/I-transport activity. Cell Physiol Biochem 18: 67-74, 2006.

Figure S1. Full-length pendrin and its C-terminal truncations p.738X, p.674X, p.584X, but not p.530X, are degraded by the ubiquitin-proteasome system. N-terminally flagged wild-type pendrin and the indicated truncations were expressed in 293 Phoenix cells (pFLAG vectors) for 48 h. (A) The whole cell lysates were probed with anti-FLAG and anti-calregulin antibodies (left panel). In an independent experiment, the cells were incubated with 1 μM MG132 for 16 h to increase the abundance of pendrin truncations, and the whole cell lysates (20 μg total proteins) were submitted to deglycosylation before western blotting (right panel). The smears on the top of the main bands in the left panel were absent in the right panel and, thus, correspond to glycosylated pendrin. Therefore, both the un-glycosylated and the glycosylated proteins (the main band plus the smear) were considered for densitometry in panel S1B and Fig. 2F. (B) Original western blot and densitometry of whole cell lysates from cells incubated with 1-10 μM MG132 or the vehicle (0.01% DMSO) for 16 h. Data are from 3-6 independent experiments. $^{*}P<0.05$ compared with wild-type, one-way ANOVA with Dunnet's post-test.

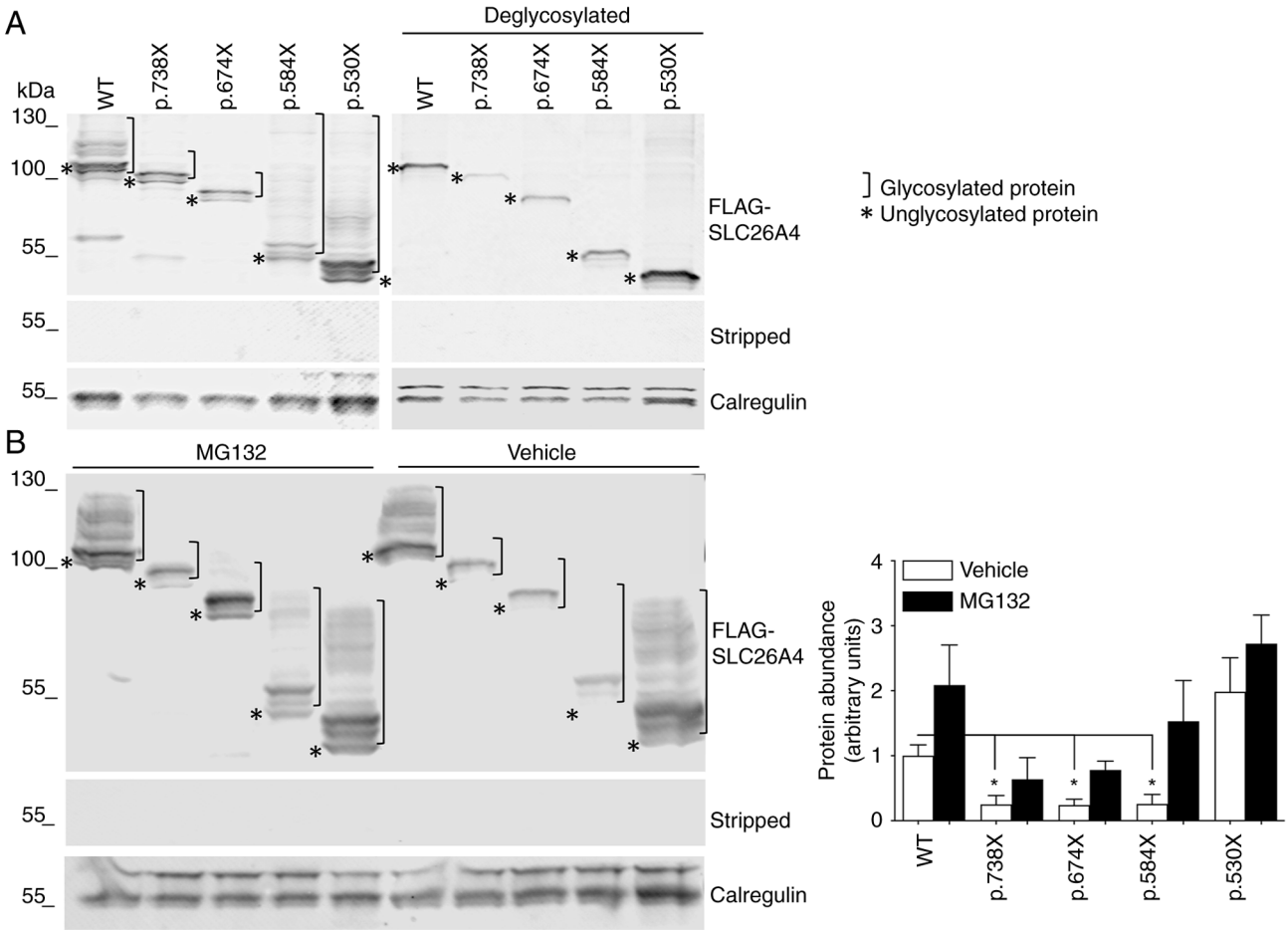

Figure S2. Bortezomib, carfilzomib and delanzomib increase total protein levels of wild-type pendrin and its variants. HeLa cells were transfected for 72 h with pEYFPN1 vectors encoding wild-type or mutant SLC26A4-EYFP and incubated with 1 μM bortezomib, carfilzomib, delanzomib, or their vehicle (0.01% DMSO) for 16 h. Total expression levels of pendrin variants were determined by quantitative imaging and normalized for those of the wild-type. ***P<0.001 and **P<0.01 compared with vehicle (two-tailed, unpaired Student's t-test). Data are from 3 independent experiments with n=6 each. n corresponds to whole imaging fields. WT, wild-type.

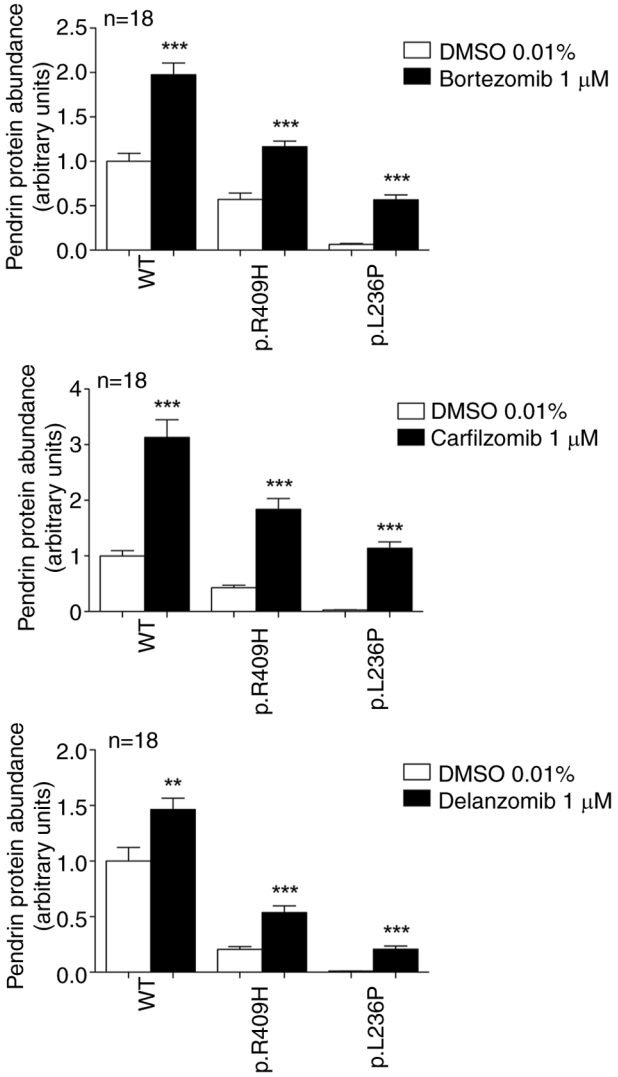

Figure S3. Bortezomib rescues the function of pathogenic pendrin variants. 293 Phoenix cells were co-transfected for 48 h with pTARGET vectors encoding the wild-type or mutant pendrin or an empty vector and the iodide sensor EYFP H148Q:I152L and incubated with bortezomib (1-10 μM) or the vehicle (0.01-0.1% DMSO) for 6-16 h. Ion transport activity was determined with a fluorometric method and the iodide influx was expressed as the % decrease of the intracellular fluorescence. ***P<0.001, **P<0.01 and *P<0.05 compared with vehicle (two-tailed, unpaired Student's t-test). Data are from 3 independent experiments with n=6 each. n corresponds to a well of a 96-well plate. WT, wild-type.

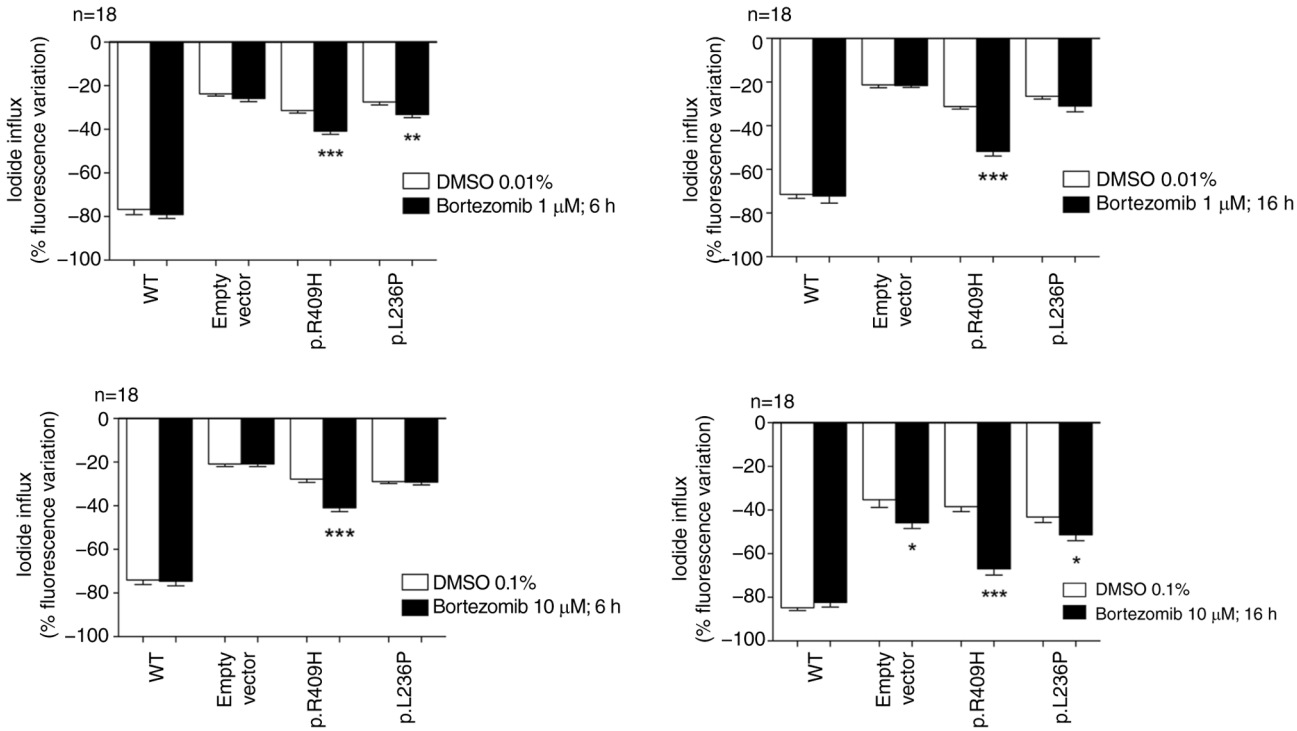

Figure S4. Carfilzomib rescues the function of pathogenic pendrin variants. 293 Phoenix cells were co-transfected for 48 h with pTARGET vectors encoding the wild-type or mutant pendrin or an empty vector and the iodide sensor EYFP H148Q:I152L and incubated with carfilzomib (1-10 μM) or the vehicle (0.01-0.1% DMSO) for 6-16 h. Ion transport activity was determined with a fluorometric method and the iodide influx was expressed as the % decrease of the intracellular fluorescence. ***P<0.001 and *P<0.05 compared with vehicle (two-tailed, unpaired Student's t-test). Data are from at least 3 independent experiments with n=6 each. n corresponds to a well of a 96-well plate.

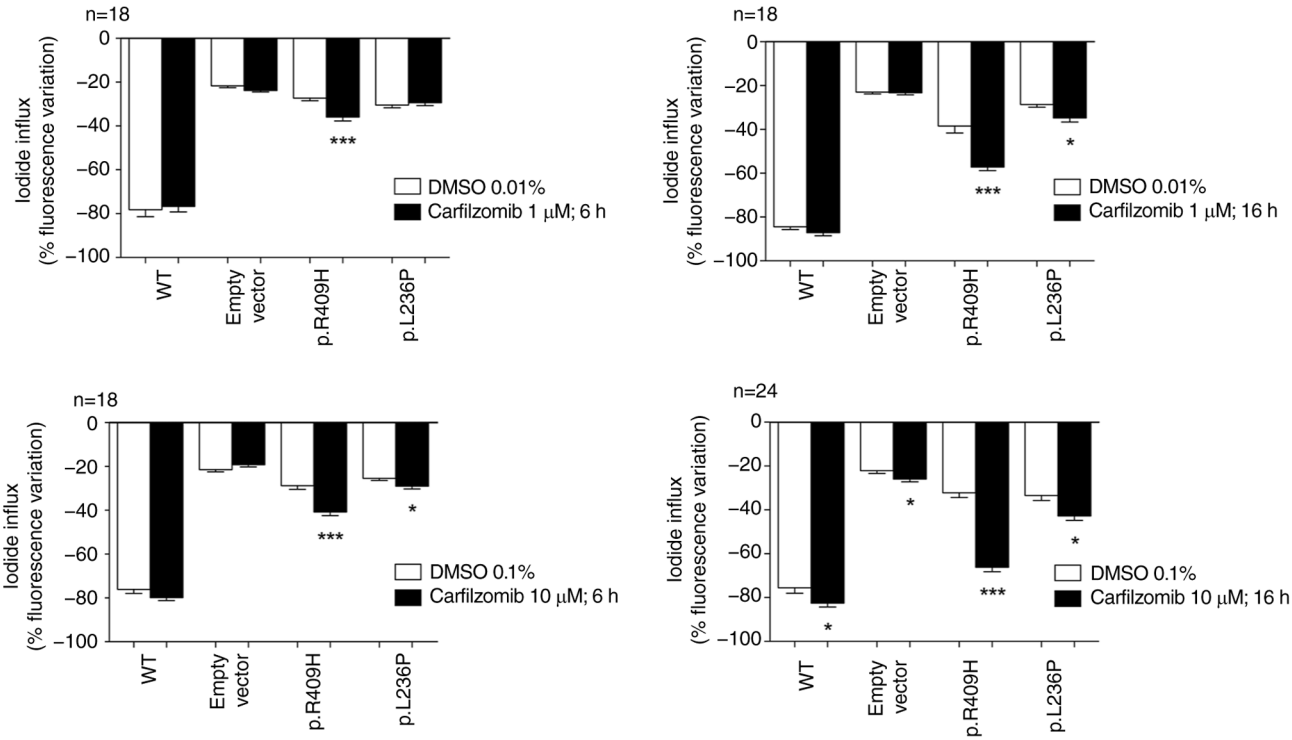

Figure S5. Delanzomib rescues the function of pathogenic pendrin variants. 293 Phoenix cells were co-transfected for 48 h with pTARGET vectors encoding the wild-type or mutant pendrin or an empty vector and the iodide sensor EYFP H148Q:I152L and incubated with delanzomib (1-10 μM) or the vehicle (0.01-0.1% DMSO) for 6-16 h. Ion transport activity was determined with a fluorometric method and the iodide influx was expressed as the % decrease of the intracellular fluorescence. ***P<0.001, **P<0.01 and *P<0.05 compared with vehicle (two-tailed, unpaired Student's t-test). Data are from at least 2 independent experiments with n=6 each. n corresponds to a well of a 96-well plate. WT, wild-type.

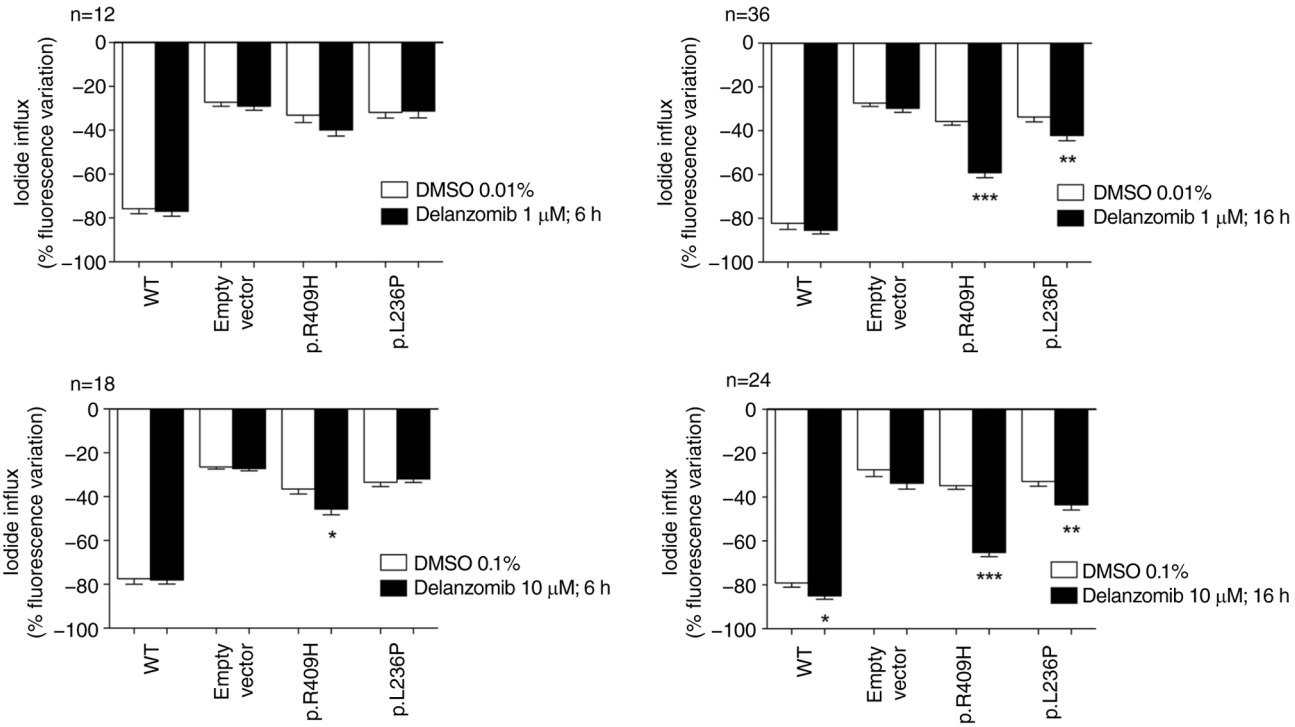

Figure S6. Carfilzomib, bortezomib and delanzomib (1-10 μM) decrease cell metabolic activity with no reduction of cell density. 293 Phoenix cells were incubated with carfilzomib, bortezomib, or delanzomib (1-10 μM) or their vehicle (0.01-0.1% DMSO) for 6-16 h. (A-D) Cell viability was measured with the CellTiter 96® AQueous One Solution Reagent in six replicate wells for each condition. (E) The cell density was determined by DAPI staining. Data are from 3 independent experiments with n=4 each. n corresponds to the wells of a 24-well plate. ***P<0.001 compared with vehicle, one-way ANOVA with Bonferroni's post hoc test.

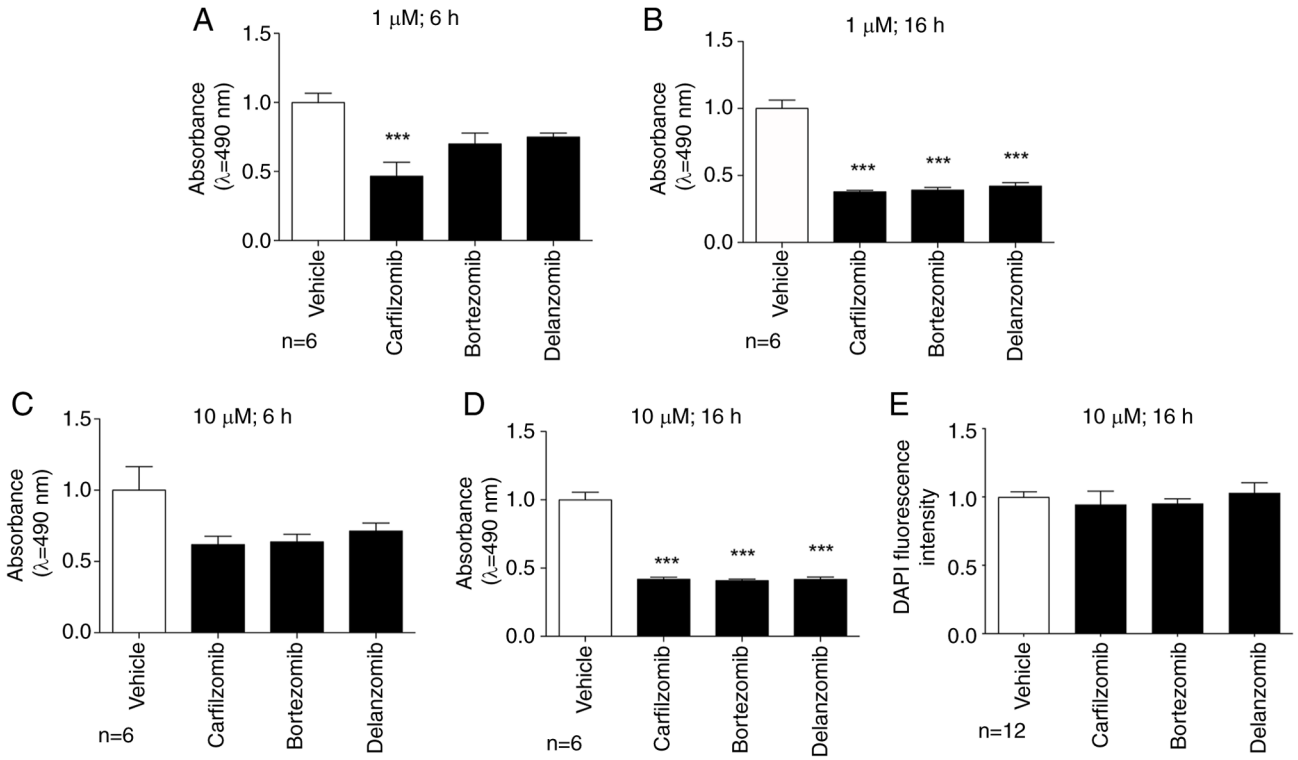

Figure S7. Lumacaftor, elexacaftor, tezacaftor, rapamycin and ataluren do not rescue the function of pathogenic pendrin variants. 293 Phoenix cells were co-transfected for 48 h with pTARGET vectors encoding the wild-type or mutant pendrin or an empty vector and the iodide sensor EYFP H148Q:I152L and incubated with lumacaftor, elexacaftor, tezacaftor, rapamycin, ataluren or their vehicle (DMSO) for 24 h. Ion transport activity was determined with a fluorometric method and the iodide influx was expressed as the % decrease of the intracellular fluorescence. *P<0.05 compared with vehicle (two-tailed, unpaired Student's t-test). Data are from 1-2 independent experiments with n=6 each. n corresponds to a well of a 96-well plate. WT, wild-type.